Water Supply

IWA PUBLISHING

Water Supply Vol 22 No 3, 2883 doi: 10.2166/ws.2021.428

Experimental studies of iron transformations kinetics and autocatalysis during its physicochemical removal from underground water

S. Yu Martynov [a,*] and V. L. Poliakov[b]

[a] Department of Water Supply, Sewerage and Drilling, National University of Water and Environmental Engineering, 11 Soborna street, Rivne, Ukraine
[b] Department of Applied Hydrodynamics, Institute of Hydromechanics of National Academy of Sciences of Ukraine, 8/4 Maria Kapnist street, Kyiv, Ukraine
*Corresponding author. E-mail: s.y.martynov@nuwm.edu.ua

SYM, 0000-0002-3136-243X

ABSTRACT

The mathematical model of physicochemical iron removal from groundwater was developed. It consists of three interrelated compartments. The results of the experimental research provide information in support of the first two compartments of the mathematical model. The dependencies for the concentrations of the adsorbed ferrous iron and deposited hydroxide concentrations are obtained as a result of the exact solution of the system of the mass transfer equations for two forms of iron in relation to the inlet surface of the bed. An analysis of the experimental data of the dynamics of the deposit accumulation in a small bed sample was made, using a special application that allowed selection of the values of the kinetic coefficients and other model parameters based on these dependencies. We evaluated the autocatalytic effect on the dynamics of iron ferrous and ferric forms. The verification of the mathematical model was carried out involving the experimental data obtained under laboratory and industrial conditions.

Key words: autocatalysis, experiment, iron removal, kinetic coefficients, model, rapid filter

HIGHLIGHTS

- Foam polystyrene filters are widely used in the water treatment practice.
- The dependences were obtained for the concentrations of two iron forms at the inlet.
- Kinetic, capacity coefficients wear established using experiments, the dependences.
- Autocatalysis essential for iron removal was accounted for using empirical functions.

INTRODUCTION

Water is an essential condition for human existence, health and activity. It has a pronounced social significance, as a sufficient amount of water of the appropriate quality is one of the main factors that ensures safe living conditions and a sustainable development of the state (Twort *et al.* 2006). However, human activity has a negative impact on the environment, including water resources, which leads to significant water pollution and exhaustion (Deng *et al.* 2013). It is anticipated that half of the world's population will experience a water shortage by 2025. Generally, people prefer underground water (artesian, spring and subsurface) when choosing a source of water supply. Groundwater is the main source of drinking water in many countries around the world (Sharma 2009; Madhukar *et al.* 2013).

Ukraine is a country with medium natural water resource. The estimated resources of Ukraine groundwater are about 61.7 million $m^3 \cdot day^{-1}$, according to the regional assessment data (Prymushko 2018). The distribution of the groundwater resources across the territory of the country is rather uneven due to the different geological and structural, physical and geographical conditions in different regions. The amount of the underground water available per capita varies within the range of 0.3–5.0 $m^3 \cdot day^{-1}$ (Tugay *et al.* 2004). Most of the resources are concentrated in the northern and north-western parts of the country, which are characterized by favourable conditions for the formation of a large volume of groundwater. Therefore, practically the entire rural population of the northern, western, north-eastern and some other regions of Ukraine uses water from underground sources (Orlov *et al.* 2017). At the same time, only a small part of groundwater complies with the modern drinking water standards. Usually the vast majority of the protected underground sources have an increased iron concentration, less

often there is an increased concentration of hydrogen sulphide, ammonium, manganese, salts of rigidity, mineralization, etc. (Tekerlekopoulou & Vayenas 2008).

Iron is a necessary element for human well-being and the healthy development of children (Sun *et al.* 2021). However, the high iron concentration makes water rusty in colour, and gives it an unpleasant metallic taste, causes overgrowth of water supply networks and water supply armature, causes defects in the manufacturing of textiles, paper, food and so on. (Chaturvedi & Dave 2012; Elsehly *et al.* 2016; Galangashi *et al.* 2021; Ma *et al.* 2021). A poor understanding of the importance of the problem of an excessive iron content and the associated need for iron removal from water can cause the deterioration of people's health and the development of chronic diseases, decrease in people's work productivity and human life duration.

Iron in natural water can exist in the forms of ferrous and ferric ions, colloids of inorganic and organic (bacterial) origin (Water Treatment Handbook 2007). These forms substantially affect the selection of the iron removal method, which it is advised should be determined by testing of iron removal from water directly near the source of water supply. The existing methods of iron removal from water can be classified as non-reagent, reagent, ion exchange, membrane and biochemical (Scholz 2016; Du *et al.* 2017; Orlov *et al.* 2017; Luong *et al.* 2018; Marsidi *et al.* 2018). The non-reagent methods of iron removal from water are used very often because they are more economical and easier to operate (Kouzbour *et al.* 2017). Some simple calculation methods were developed for them (Stiriba *et al.* 2017; Vries *et al.* 2017), but they do not take into account a number of important features such as the nonlinear effects of the mass transfer, autocatalytic process, deposit consolidation, etc.

Our long-term study experience of iron removal from water under laboratory and industrial conditions at the operating iron removal plants in Ukraine, including our water stations of iron removal with foam polystyrene filters, allowed us to develop a mathematical model of physicochemical removal of the groundwater iron, which was outlined previously. The developed mathematical model consists of three interconnected compartments (Poliakov & Martynov 2021).

The first compartment primarily includes a system of equations relative to the concentrations of the dissolved (C_a), adsorbed (S_a) ferrous iron:

$$V\frac{\partial C_a}{\partial z}+\frac{\partial S_a}{\partial t}+K_d\,S_a+k_s\,C_a=0 \tag{1}$$

$$\frac{\partial S_a}{\partial t}=k_a f_a(S_h)\,(S_{ma}-S_a)\,C_a-K_d\,S_a \tag{2}$$

and the boundary, initial conditions:

$$z=0,\;\; C_a=C_{a0} \tag{3}$$

$$t=0,\;\; S_a=S_a^0 \tag{4}$$

where V[m·h^{-1}] is the filtration rate; z[m] is the coordinate on the vertical axis; t[h] is the filtration time; K_d[h^{-1}], k_s[h^{-1}] are the coefficients of oxidation rates Fe^{2+} in adsorbed and free state; k_a[m^3·g^{-1}·h^{-1}] is the reduced adsorption rate coefficient for Fe^{2+}; f_a[–] is the autocatalytic function describing adsorption Fe^{2+} at the newly formed deposit; S_h[g·m^{-3}] is the volumetric concentration of deposited hydroxide particles; S_{ma}[g·m^{-3}] is the adsorption capacity of the filter medium relative to Fe^{2+} ions.

The second compartment contains a system of equations similar to (1), (2) with respect to the concentrations of the suspended (C_h) and deposited (S_h) hydroxide particles:

$$V\frac{\partial C_h}{\partial z}+\frac{\partial S_h}{\partial t}-K_d\,S_a-k_s\,C_a=0 \tag{5}$$

$$\frac{\partial S_h}{\partial t}=k_h f_h(S_h)\,(S_{mh}-S_h)\,C_h+K_d\,S_a \tag{6}$$

and conditions:

$$z = 0,\ \ C_h = C_{h0} \tag{7}$$

$$t = 0,\ \ S_a = S_a^0(z) \tag{8}$$

where $k_h[m^3 \cdot g^{-1} \cdot h^{-1}]$ is the reduced coefficient of the settling rate of the hydroxide particles; $f_h[–]$ is the autocatalytic function describing the immobilization of the suspended particles onto the deposit; $S_{mh}[g \cdot m^{-3}]$ is the adsorption capacity of the filter media relative to the indicated particles (dirt-holding capacity).

The third compartment consists of the equations of motion (Darcy's law), the hydraulic resistance of a bed and the deposit state (Poliakov & Martynov 2021).

An exact solution of the system of the mass transfer equations was obtained for two forms of iron in relation to the inlet surface of a medium. That allows substantiating of the legitimacy of the application of the dynamic averaging method for solving a general problem of physicochemical iron removal from groundwater. The exact solution to the basic problem was obtained without considering autocatalysis. At the same time, it is necessary to experimentally determine and analyze its coefficients and parameters, to provide adequate experimental data and theoretical results using the proposed mathematical model. Special attention was given to the determination of the deposit composition (the ratio of the mineral component to the bound water), and the hydrodynamic stability depending on the deposit age (polymerization and dehydration). The solutions to these problems will allow establishment of the rational construction and technological parameters of iron removal from water using rapid filters. The collected materials will be presented in two articles taking into account the large amount of accumulated data, the specifics of research in both directions (water clarification and flow in a porous contaminated medium). This article provides the research data on the information support for the first two compartments of the mathematical model, which are related to the processes of water clarification.

METHODS

Numerous studies of physicochemical iron removal from water under laboratory and industrial conditions at the iron removal plants operating in Ukraine were conducted to obtain the initial information for the development of a mathematical model of physicochemical iron removal from groundwater and establish the parameter values and perform the verification of the mathematical model. The plants for iron removal with a 'heavy' medium (zeolite, granite gravel) and also with a 'floating' medium (foam polystyrene) which were constructed according to our recommendations were studied over many years of our research activity. It should be noted that foamed polystyrene as a rapid filter medium was firstly proposed for use at the Department of Water Supply, Sewage and Drilling at the National University of Water and Environmental Engineering (Rivne, Ukraine). Foam polystyrene filters are widely used in the water treatment worldwide due to the design and technological advantages (Orlov *et al.* 2016). The iron removal plants under our consideration satisfy the drinking water needs of cities, towns, villages and individual cottages with different productivity in the range from 4 to 40,000 $m^3 \cdot day^{-1}$.

Laboratory plants

The experimental studies of iron removal from water were conducted on a macroscale. The plants for the non-pressure iron removal research (Figure 1) consisted of a filtration column, a filter rate regulator, a piezometer shield, a dosage unit with the sulfuric acid iron solution and limewater. The disassembled filtration column is made of four pipes Ø150 mm high, each of 0.4 m. Two of them are made of plexiglas and the other two are made of polypropylene. The cone with the nipple of aeration water connection and the flushing pipe were connected to these pipes from the bottom, and the steel tank Ø500 mm was connected to these pipes on the top. Thanks to this plant design it was possible to observe visually the processes taking place in the sublattice space and to change its height. There were 4 nipples arranged by the height of the filtration column to connect the piezometers on one side and 5 sample extractors arranged in this way every 20 cm on the other side. The water amount collected by the samplers did not exceed 5% of water passing through the filtration column. The head losses in the filtration column were controlled by a shield of piezometers.

The plant was operating as follows: water from the city water supply was directed into the tank to a constant level, then to the mixer through the regulating valve, where it was mixed with an iron solution. The iron solution was prepared using iron sulphate (II), which was dissolved in distilled water. The adjustments were made to provide uniformity for the iron solution supply at each point of time before each filter run. The necessary solution consumption was made possible by using a clamp,

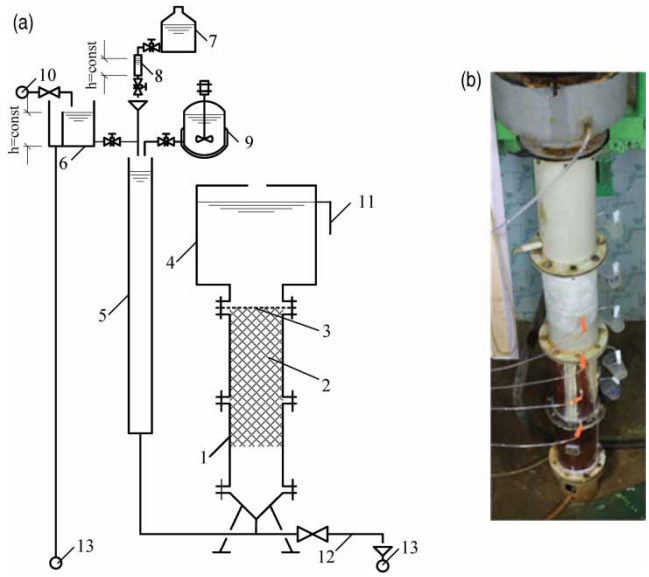

Figure 1 | Experimental plant for study of iron removal from water: (a) scheme; (b) plant photo; 1. Filtration column, 2. Foam polystyrene medium, 3. Detained grid, 4. Above filter space (washing volume), 5. Filter rate controller, 6. Tank with a constant level, 7. Marriott vessel with iron sulphate solution, 8. Cylinder with a constant level, 9. Marriott vessel with mechanical mixer and limewater, 10. City water supply, 11. Outflow pipe for water after iron removal (filtrate), 12. Pipe for outflow of dirty washing water, 13. Sewerage.

which was placed after it at a constant height of the liquid in cylinder 8. The uniformity of the iron solution losses was ensured by maintaining a constant level of liquid in cylinder 8 with a clamp placed after tank 7. It is necessary to conduct the liming of water because air oxygen does not oxidize iron sulphate well. The limewater was poured into tank 9 for this purpose. A mechanical mixer was used to prevent deposition of the lime particles at the bottom of the tank. The necessary expenditure of lime solution was controlled by a valve. The lime solution was fed directly to the filter rate controller. The reagents were mixed with water in the filtration rate regulator**.** Then the water was directed into the sub-filter space and foam polystyrene medium. The water after iron removal was collected in the above filter space. The medium backwashing was carried out with iron removal water from the above filter space by opening the valve on pipe 12.

The efficiency of iron removal from water and the increase in head losses were investigated in media of different granulometric composition. The filter medium height was set as 0.8–1.3 m during laboratory studies. As a rule, the filtration rate, the iron concentration, and the head losses in the medium were determined during the experiments after 1–2 hours. Readings were taken for these indicators every 15 min or less at short filter runs or when approaching the end of the filter run. The filtration rate was supported as constant throughout the filter runs. As a rule, the water physicochemical parameters were determined in the middle of each filter run.

The careful backwashing of freshly prepared medium and hydro classification by descending water flow was carried out for 10–15 minutes after it had been supplied to the filtration column. Then 1–4 testing filter runs were ‘ripening’ of the medium. The indicators of water quality were determined according to the requirements of the National Standard of Ukraine ‘Drinking Water. Requirements and methods of quality control’ and reference literature. The mass iron concentration was found according to the MIU No. 081/12–0175-05 Surface, underground and return water. The iron mass concentration was measured by the general photo colorimetric method with rhodanide.

The studies were conducted in a laboratory to obtain model parameters that modelled the process of iron removal in the elementary bed of a foam polystyrene medium. They were carried out by filtering the mixture of two forms of iron and also separately ferrous and ferric iron. The scheme of the experimental plant is shown in Figure 2.

The water with high iron concentration (model solution) was prepared using iron sulfate. The expenditure was set by control clamp 4 at an average water level in Marriot vessel 3. When the water level would decrease in Marriot vessel 3 (baring of the minimum level sensor) controller 10 turned on pump 9 Marriot vessel 3 (baring of the minimum level sensor). Marriot vessel 3 was filled with the model solution until the maximum water level sensor closure. Then the pump was turned off. Thus, the same water consumption was ensured throughout each filter run. Filter 8 with sodium thiosulphite is installed to prevent air oxygen ingress into the capacity 7, with a ferric iron model solution.

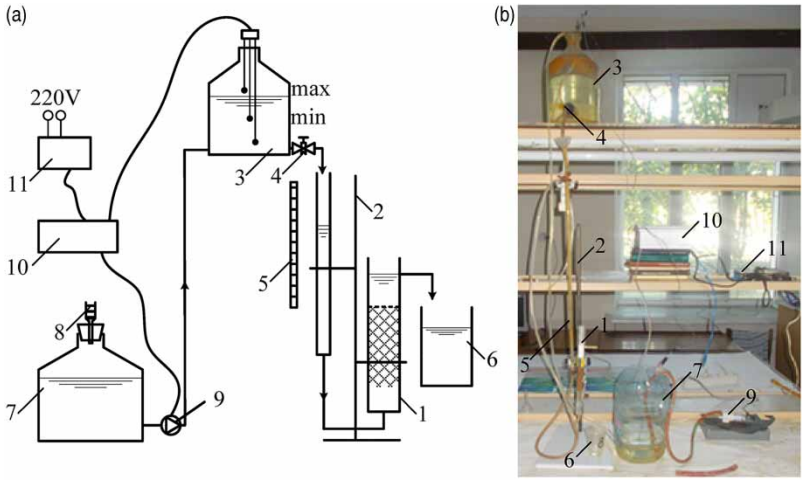

Figure 2 | **Scheme of the experimental plant**: (a) scheme; (b) plant photo; 1. Filtration column with foam polystyrene medium, 2. Laboratory tripod, 3. Marriott vessel, 4. Control clamp, 5. Measuring line, 6. Tank for filtrate, 7. Tank with model solution of ferric iron, 8. Absorption air oxygen filter, 9. Pump, 10. Controller, 11. Power supply unit.

Industrial research

The industrial researches of physicochemical iron removal from underground water at the filter with a zeolite medium were carried out at the iron removal plant of a railway station with a productivity of 1,000 $m^3 \cdot day^{-1}$ (Figure 3). The iron removal from water provided air introduction via the compressor into the underground water pressure pipeline with the subsequent filtration on pressure filters with zeolite medium. The filtrate was disinfected using bactericidal lamps. Then it was accumulated in the water pressure tower. After that it was sent to the water supply network.

The results of our research on the filtration structures with gravel medium were implemented at the Gorbakovsky water intake complex. The complex included a water intake wells compartment, an aeration and filtration structures compartment and a backwashing waters treatment and deposit compartment. The daily productivity of the water intake complex was 41,000–44,000 $m^3 \cdot day^{-1}$. Water treatment was carried out by 16 non-pressure filters which were located in two plants, 8 pcs in each plant. Filters were loaded with crushed granite. The thickness of the filter medium was about 1.9 m. The water aeration occurred in two stages. At first, the water outflows at the height of 0.5 m at the inlet chamber, common for each of the 4 filters and then it outflows from the tray aerator in addition, which was located in each filter. Indicators of water quality at the inlet and outlet from the plant and for individual filters, the dynamics of head losses in the medium were controlled during the process under consideration. The water expenditure was determined using a Panametrix portable flowmeter. The soluble oxygen concentration in water was determined by the Winkler method. Placing the water samples in oxygen cups using a siphon tube to exclude the possibility of air entraining into the water was being examined.

We introduced a scheme of physicochemical iron removal from water with non-pressure foam polystyrene filters for water preparation for the economic and drinking needs of Goscha village (Figure 4(a)) with the estimated productivity of 850

Figure 3 | Iron removal plant with the pressure zeolite filters: (a) general view of the station; (b) filtration room.

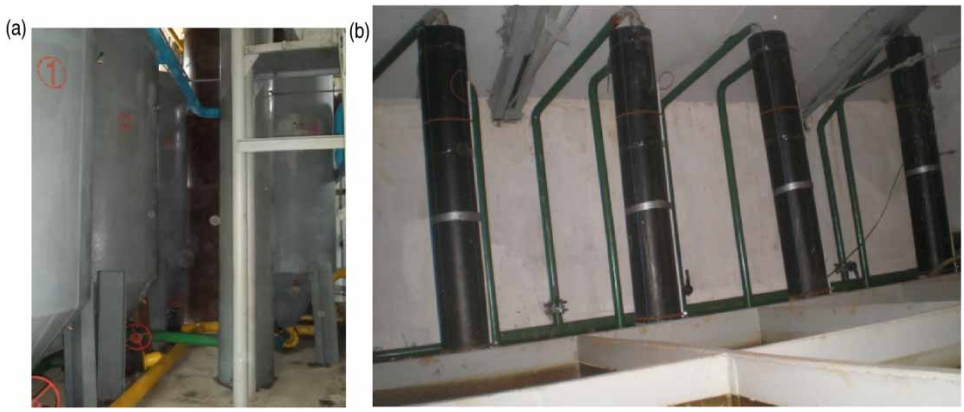

Figure 4 | Nonpressure foam polystyrene filters with the ascending filtration: (a) around at the plan; (b) cellular type.

$m^3 \cdot day^{-1}$. The technological scheme was as follows. Artesian water enters the aerator, where the water saturation by air oxygen and partial removal of dissolved gases (carbon dioxide and hydrogen sulphide) take place. Then water enters the air separator and through the aeration water pipeline goes to the bottom of the four filters. The lower parts of the filters were shaped as a cone to prevent the clogging of the holes of the tubular drainage system. The iron extraction process is occurring directly in the medium, simultaneously with the ferrous iron oxidation. The filtration is carried out by an ascending flow through the foam polystyrene medium of industrial production with granules of increasing size. A special structure was designed to hold foam polystyrene in a flooded state. It consists of a support frame and a grille, with a stainless net fixed between them. The backwashing of the foamed polystyrene medium was performed alternately using water from the common above filter space by opening only one latch on the washing pipeline. The filters are switched alternately for backwashing.

Mounted on a common piezometer shield from each filter, piezometric tubes were connected to control the operation of iron removal equipment. The samplers were arranged on the second filter by their height to study step by step effectiveness of iron removal from water. Water samples were taken from the inlet (initial) water to determine the iron forms in the sub-filter space of the filter and the filtrate, which were preserved by a generally accepted methodology.

We have implemented and studied the operation of the water preparation plants for the paper factory needs with the productivity of 90 $m^3 \cdot h^{-1}$ (Figure 4(b)) using the same scheme.

The tower technological scheme for iron removal from water was developed. It was implemented and researched in 8 Ukrainian sites in Rivne, Khmelnytsky and Vinnytsia regions with a productivity of 4–15 $m^3 \cdot h^{-1}$ (Figure 5). The placement of all total water treatment equipment inside the operating steel water towers is a characteristic of such schemes that significantly reduces capital costs for the construction of the iron removal plants.

RESULTS AND DISCUSSION

Kinetic and capacity coefficients of compartments Fe^{2+} and Fe^{3+}

The dynamics of the physicochemical groundwater iron at the inlet section of the filter medium was analyzed by analytical methods in the first article of our series (Poliakov & Martynov 2021). Firstly, the filter material is contaminated here at the highest rate and its throughput sharply decreases as a result. Second, we succeeded in deriving dependencies which strictly describe immobilization of two iron forms taking into account the autocatalytic effect precisely in this section. The obtained results can be considered as a standard when carrying out complex studies and are able to benefit because:

- allows estimation of the significance of specific (nonlinear) effects caused by autocatalysis, limitation of the dirt-holding capacity of the medium in relation to ferrous iron and iron hydroxide;
- permits identification of the errors introduced in the calculation dependencies due to the use of approximate techniques and methods for solving the applied problems;
- are a reliable basis for the experimental data processing to obtain the characteristic values of the model coefficients and the approbation of the calculation dependencies.

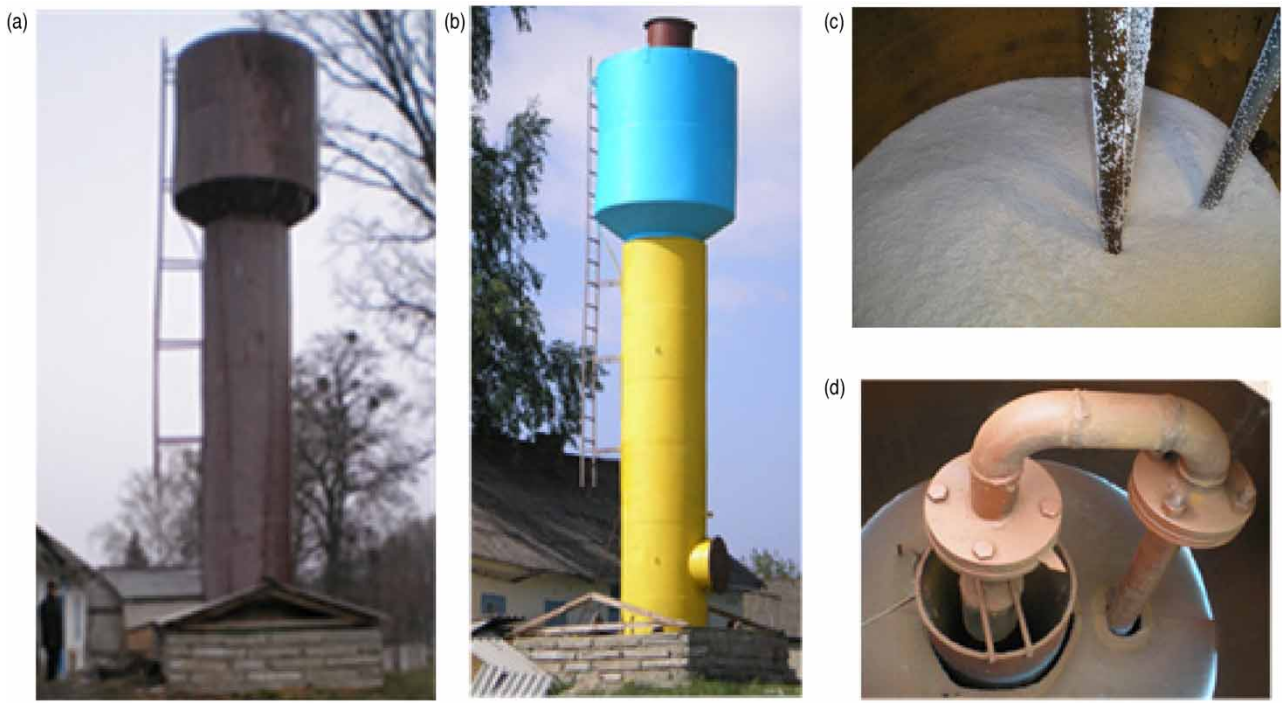

Figure 5 | Tower plant for iron removal from water: (a) before reconstruction; (b) after reconstruction; (c) foam polystyrene medium; (d) aeration and degasification.

The corresponding mathematical model for the selected section represents a substantially simplified version (mathematically but not physically) of the general model of the physicochemical iron removal with simplified aeration. In this case only the concentrations of the adsorbed ferrous S_{a0} and sorbed hydroxide (in a general sense) S_{h0} serve as the calculation subject. The basic model of mass transfer for two *Fe* forms, which is taken for the inlet cross section, includes the next system of nonlinear kinetic equations:

$$\frac{dS_{a0}}{dt} = k_a \cdot f_a(S_0) \cdot (S_{ma} - S_{a0}) \cdot C_{a0} - K_d S_{a0} \tag{9}$$

$$\frac{dS_{h0}}{dt} = k_h \cdot f_h(S_0) \cdot (S_{mh} - S_{h0}) \cdot C_{h0} + K_d S_{a0} \tag{10}$$

the initial conditions are joined to it:

$$t = 0, \;\; S_{a0} = S_{a0}^0, \;\; S_{h0} = S_{h0}^0 \tag{11}$$

The dependences for the concentrations of ferrous iron oxide and deposited hydroxide are obtained as a result of the exact solution of the system (9), (10) with the initial conditions (11). Analysis of the experimental data on the deposit accumulation dynamics in the medium elementary volume was performed. A special application was used based on these dependencies. It made possible selection of the kinetic parameters values using the nonlinear simplex method. The function Minimize was used in MathCAD with the restriction Given. In particular, the best conformity between experimental and theoretical data was observed at such values of the coefficients in the dimensional form: $k_a = 0.45 \pm 0.04$ $\mathrm{m^3 \cdot g^{-1} \cdot h^{-1}}$, $k_h = (4.0 \pm 0.3) \cdot 10^{-2}$ $\mathrm{m^3 \cdot g^{-1} \cdot h^{-1}}$, $K_d = 0.14 \pm 0.01$ $\mathrm{h^{-1}}$, $S_{mh} = 5.0 \pm 0.4$ $\mathrm{kg \cdot m^{-3}}$ and in dimensionless form: $\overline{k}_a = (5.0 \pm 0.4) \cdot 10^{-3}$, $\overline{k}_h = (4.4 \pm 0.4) \cdot 10^{-4}$, $\overline{K}_d = (1.0 \pm 0.1) \cdot 10^{-3}$, $\overline{S}_{mh} = 1.0 \pm 0.1$. The calculation results using the above-mentioned values of the model coefficients almost coincided with the experimental studies (Figure 6). In this case, the average relative error was 4.6%.

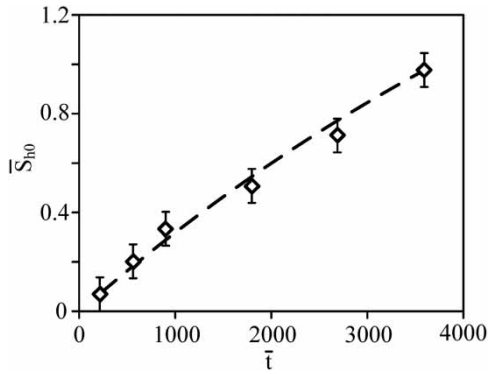

Figure 6 | Dependence $\bar{S}_{h0} = f(\bar{t})$.

The amount of the immobilized iron and its distribution by the height of the medium play an important role in the dynamics of iron removal from water. They affect both the effectiveness of iron removal from water and the growth of head losses. The role of autocatalysis becomes more prominent with the increase in the amount of immobilized iron. The autocatalytic functions $f_a(S)$, $f_h(S)$ included in (9), (10) describe this phenomenon. Hence, sorption (adsorption) of the iron compounds increases. On the other hand, the available medium resource characterizing ferrous iron ($S_{ma} - S_a$) and ferric iron ($S_{mh} - S_h$) dirt capacity decreases due to increase in the amount of immobilized iron. It slows down the iron compounds transition into the solid phase. At first, the mutual opposite effect of these two effects leads to increase in the intensity of iron compounds adhesion to the medium. Subsequently, it leads to a rapid deceleration of the process.

The following types of the ultimate concentrations of the immobilized iron should be noted:

- The maximum limiting concentration that is typical for the porous medium space with its full saturation by iron compounds, when treatment efficiency is zero. In this case, the head losses growth does not occur;
- The maximum operating concentration is typical in a case where saturation of the medium porous space by the iron compounds is not complete and is limited to one of three parameters: the time of reaching ultimate head losses, the time of the medium protection, the time to achieve critical 'strength' of the deposit. This value is the averaged dirt capacity (kg·m^{-2}) of the medium in which the filter rational parameters are provided for the specified conditions;
- The minimum operating concentration is the minimum amount of the deposit retained after backwashing in the medium to ensure the necessary iron concentration in the filtrate at the beginning of the filter run. The residual deposit in the medium after the backwashing improves the medium adsorption-catalytic properties. That in turn is accounted for by the higher values of the functions $f_a(S)$, $f_h(S)$ in the kinetic Equations (9) and (10).

Minimum and maximum operating concentrations are determined on the basis of the mathematical model of physicochemical iron removal from groundwater, which is given in the first article of this series. The laboratory plant described above was used to determine the ultimate concentration of the immobilized iron. The ultimate concentration of the immobilized iron under specified construction and technological parameters of the plant was determined using the dependence graph $S = t_f$ (here t_f is the duration of the filter run). The required value S_m is the point where the graph becomes a horizontal line (Figure 7).

Consequently, the obtained value of the maximum limiting concentration for the immobilized iron is $S_m = 5.0$ kg·m^{-3} by chemical iron. As a result of recalculation to iron hydroxide (III) we obtain:

$$S_{Fe(OH)_3} = S_m \cdot \frac{Mr(Fe(OH)_3)}{Ar(Fe)} = 5.0 \cdot \frac{103.8}{55.8} = 9.3\,\text{kg} \cdot \text{m}^{-3} \tag{12}$$

where $Mr(Fe(OH)_3)$ is the molecular mass of the iron hydroxide; $Ar(Fe)$ is the atomic iron mass.

The ratio of the maximum limiting concentration of adsorbed ferric iron to sorbed iron hydroxide is an important question too. There are 91.1% of ferric iron (Fe^{3+}) and 8.9% of ferrous iron (Fe^{2+}) in the film (on the surface of the granules) and 100% of ferric iron (Fe^{3+}) in the deposit according to Tugay *et al.* (2004). Also according to Orlov *et al.* (2017), 2–30% of the ferrous iron and 70–98% of the ferric iron are in the deposit. Therefore, the two forms of the iron ultimate concentration in the

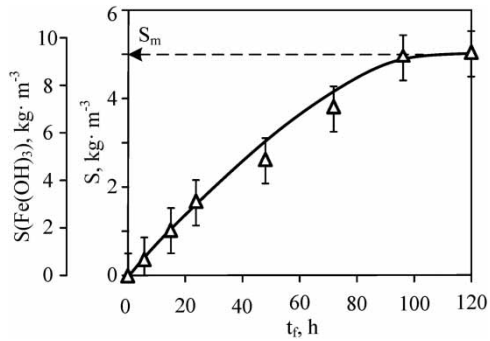

Figure 7 | Determination of the ultimate concentration of the immobilized iron.

medium of 5.0 kg·m^{-3} contain 2–30% (0.1–1.5 kg·m^{-3}) of the ferric iron (Fe^{2+}) and 98–70% (4.9–3.5 kg·m^{-3}) of the ferric iron (Fe^{3+}). It is 9.1–6.5 kg·m^{-3} in transfer to $Fe(OH)_3$.

Autocatalytic functions

The autocatalytic effect was taken into account by empirical functions f_a, f_h when modelling physicochemical iron removal. They were introduced into the kinetic equations of ferrous (9) and ferric (10) iron forms. These functions also influence the adsorption and sorption processes, noticeably reinforcing them. As a result, the acceleration of the deposit formation has occurred. The corresponding functions can be presented in the first approximation for the formal description of the autocatalytic effect in the following way:

$$f_a(\bar{S}) = (1 + \theta_a)\bar{S} \tag{13}$$

$$f_h(\bar{S}) = (1 + \theta_h)\bar{S} \tag{14}$$

where θ_a[–], θ_h[–] is a pair of corrective functional coefficients, which allow refining of the results of modelling by taking into account the autocatalysis.

It is proposed to use the functional autocatalytic coefficients, to evaluate the effluence of the noticed effect:

$$A_{a0}(\bar{t},\ \theta_a) = \frac{\bar{S}_{a0}(\bar{t},\ \theta_a)}{\bar{S}_{a0}(\bar{t},\ \theta_a \to 0)}, \quad A_{h0}(\bar{t},\ \theta_h) = \frac{\bar{S}_{h0}(\bar{t},\ \theta_h)}{\bar{S}_{h0}(\bar{t},\ \theta_h \to 0)} \tag{15}$$

They characterize the relative increase in the adsorbed ferrous iron and deposited iron hydroxide due to the indicated effect only. The results of the calculations A_{a0} based on (9)–(11) are shown in Figure 8 at such initial data: $\bar{k}_a = 0.015$, $\bar{K}_d = 0.0015$, $\bar{S}_{ma} = 1$, $\bar{C}_{a0} = 0.5$.

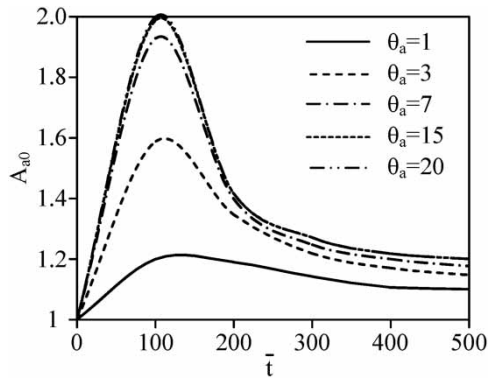

Figure 8 | Dependence $A_{a0}(\bar{t})$.

Thus, the parameter S_{ma} is served here as a scale for $\bar{S}_{a0}$. The maximum value of A_{a0} was reached at $\bar{t} \approx 120$, $\theta_a = 20$ and equalled 2.0.

Similar calculations were carried out in relation to ferric iron based on the values of the model parameters: $\bar{k}_a = 0.005$, $\bar{K}_d = 0.001$, $\bar{k}_h = 0.0005$, $\bar{k}_s = 0$, $\bar{S}^0_{h0} = 0.05$, $\bar{S}^0_{a0} = 0$, $\psi = 5000$. It was accepted that $\bar{S}_{ma} = 0.2$ because the parameter S_{mh} was used as a scale for concentrations S_{a0} and S_{h0}. The autocatalytic effect affects the accumulation dynamics of iron hydroxide less than the adsorption process. Especially, it manifests at $\bar{t} < 700$, which corresponds to the actual duration of the process of underground water filtration at the plants for physicochemical iron removal (Figure 9).

The practical estimation of the coefficients θ_a, θ_h was carried out in MathCAD on the basis of the experimental results obtained at the plant for iron removal from water with foam polystyrene filters with the productivity of 800 $m^3 \cdot day^{-1}$. The following values of the coefficients were obtained as a result of the calculations: $\theta_a = 15.0 \pm 1.5$, $\theta_h = 2.5 \pm 0.3$. The dynamics of the two forms of iron in the filtrate over time are shown in Figure 10. The calculated values are represented by lines and the experimental values by dots on this figure. The sufficient concurrence of the experimental and calculated values confirms the legitimacy of the presentation of the accepted form of the autocatalytic effect at the physicochemical iron removal from underground water.

Verification of the mathematical model of the physicochemical iron removal from groundwater using a rapid filter

The experimental data obtained under industrial and laboratory conditions were used to verify the mathematical model of the physicochemical iron removal from water. There was a comparison of the theoretical and experimental results initiated for the changes in the dynamics in the iron concentration in the filtrate over time and the height of the medium in the partially clogged medium. The values of the kinetic coefficients in the theoretical calculations are accepted based on the analysis of the experimental data of the dynamics of the deposit accumulation in a small sample of the medium given in Part 3.1.

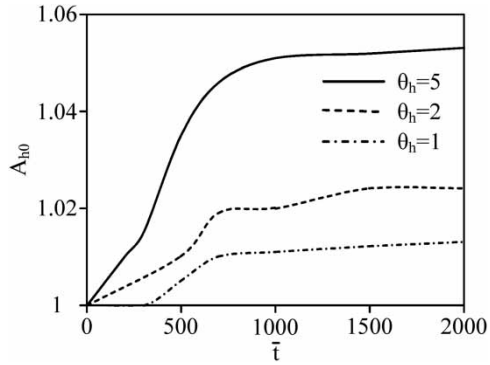

Figure 9 | Dependence $A_{h0}(\bar{t})$.

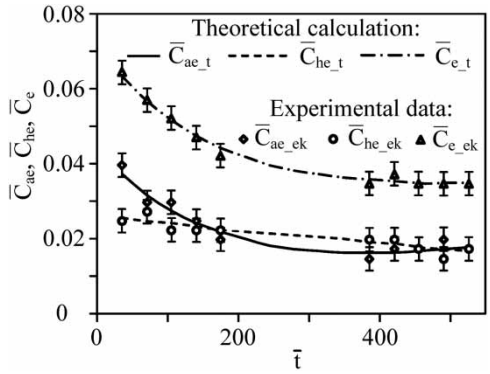

Figure 10 | Dynamics of the relative concentrations of two iron forms and their sum in the filtrate.

The results of the laboratory tests (lines) for removal of iron from water in a foam polystyrene filter with large-granule medium of industrial production and the corresponding calculation data (symbols), which were obtained theoretically, are shown in Figure 11.

In general, the calculated values are in good agreement with the experimental results.

The sorption (adsorption) coefficients depend on the basic parameters for industrial research. The parameters take into consideration the kinetics of iron removal from water, features of the autocatalytic reactions, transfer conditions and iron fixation in the solid phase. The sorption (adsorption) coefficients were determined by the formulae:

$$k_a = k_a^* \cdot (V/n)^{\varepsilon_1} \cdot (\alpha \cdot d)^{\varepsilon_2}, \quad k_h = k_h^* \cdot (V/n)^{\varepsilon_3} \cdot (\alpha \cdot d)^{\varepsilon_4} \tag{16}$$

and iron oxidation in the solid and liquid phases:

$$K_d = K_d^* \cdot S_{O2} \cdot 10^{2pH}, \quad k_s = k_s^* \cdot C_{O2} \cdot 10^{2pH} \tag{17}$$

where k_a^*, k_h^* are the kinetic coefficients that depend on the physicochemical indicators of the quality of water entering the filter medium and the deposit properties; K_d^*, k_s^* are the kinetic coefficients that depend on the physicochemical indicators of the quality of water entering directly into the medium; C_{O2}[g·m^{-3}], S_{O2}[g·m^{-3}] are the concentrations of the dissolved oxygen in the liquid phase and on the deposit surface; n[–] is the current medium porosity; d[m] is the diameter of a grain in the medium; α[–] is the grain form factor; pH[–] is the hydrogen index; ε_1-ε_4[–] are the empirical coefficients depending on the delivery conditions and iron fixation in the solid phase (deposit).

The coefficients K_d^*, k_s^* in the case of the iron oxidation in a more complex way (the presence of the reaction catalysts or inhibitors in the water) should be specified taking into account the concentration of these substances in accordance with oxidation chemistry. The simplest way of water aeration (water outflow from the height of 0.5 m) provides the concentration of dissolved oxygen in water of 5–6 g·m^{-3}, which is several times larger than the stoichiometric need to oxidize a small amount of iron. The concentrations of dissolved oxygen and hydrogen ions can be considered almost constant with sufficient values of the hydrogen index and water alkalinity. Therefore, the use of the coefficients K_d and k_s were justified without taking into account these changes. The coefficients ε_1-ε_4 were determined using the experimental data at the plants with different granulometric composition of foam polystyrene medium for the filtration rates of 3–8 m·h^{-1}. We used the specially developed application in MathCAD with Minimize function and Given limitations. The minimum value of the approximation criterion was served as the criterion for determining the optimal values of the required coefficients. Each coefficient ranged from -2 to $+2$. The following values of the coefficients were obtained: $\varepsilon_1 = 0.3$, $\varepsilon_2 = -1.5$, $\varepsilon_3 = 0.3$, $\varepsilon_4 = -1.5$.

Figure 12 allows comparison of the concentrations of the iron forms in the filter bed. The comparison of the changes in the concentrations of iron in the filter bed is illustrated in Figure 12 at two points in time, for iron removal from water at an industrial plant for water treatment with foam polystyrene filters at the following initial data: $[C_{O2}] = [S_{O2}] = 5$ g·m^{-3}, $d = 2.8$ mm, $L = 1.1$ m, $C_0 = 1.15$ g·m^{-3}, $C_{a0}/C_0 = 0.6$.

The calculation results are in good agreement with the experimental data and the average relative error does not exceed 8%.

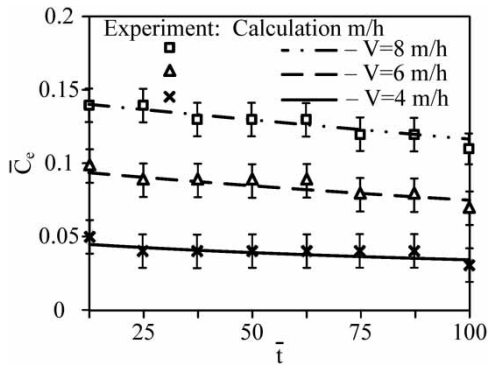

Figure 11 | Dynamics of the relative total iron concentration in the filtrate over time at different filtration rates.

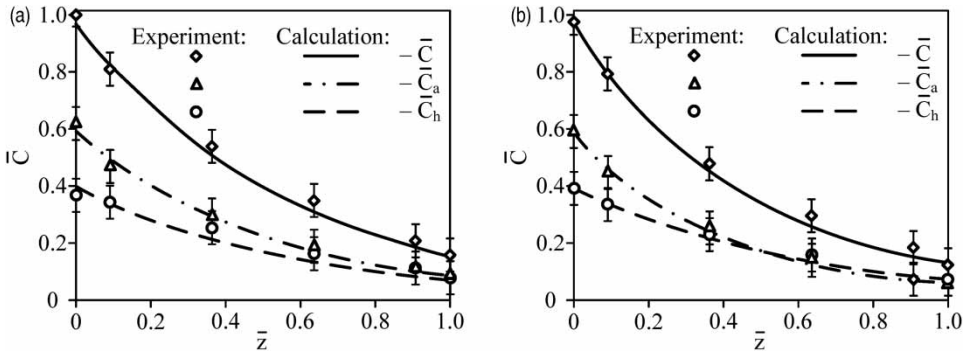

Figure 12 | Distribution of the relative concentration of the iron forms by the height of the medium in the liquid phase during the filtration run: (a) t = 0.5 h; (b) t = 15.0 h.

CONCLUSIONS

A considerable part of the groundwater resources has a high *Fe* concentration, which negatively affects the population life. Multiple experimental and theoretical researches were performed to solve this problem, various technological schemes and relatively simple calculation methods were developed. However, a number of important effects were not taken into account, such as the nonlinear effects of mass transfer, the autocatalytic process, the features of the deposit consolidation, and so on. The physicochemical iron transformations play a key role in the practice of iron removal from water, because they are directly responsible for the iron removal. Using practical long-term experience we have developed a mathematical model for the physicochemical iron removal from underground water, which consists of three interrelated compartments describing the transfer, adsorption and oxidation of ferrous iron, the transfer and sorption of ferric iron (compartments of ferrous and ferric iron) and the hydraulic compartment that describes the flow with the suspended particles through the clogged granular filter medium. We have conducted careful studies of the process of iron removal from water under laboratory and industrial conditions at the operating plants for iron removal in Ukraine for information support of the mathematical model of physicochemical iron removal from groundwater. The analysis of the experimental data was performed relative to the dynamics of the deposit accumulation in a small sample of the medium, which allowed selection of the value of the kinetic parameters using the nonlinear simplex method. The capacitive coefficients were estimated for *Fe* ferrous and ferric compartments as to the inlet section using the experimental data and scientific literature. The freshly retarded deposit increases the efficiency of iron removal using the rapid filters. The autocatalytic functions were used to estimate the impact of the specified effect. The calculations showed that the autocatalytic effect is primarily demonstrated at $\bar{t} < 700$ which corresponds to the real duration of groundwater filtration at the plants for physicochemical iron removal. The values of the autocatalytic coefficients for the kinetic equations of two *Fe* forms were determined using experimental data and specially designed application. The verification of the mathematical model was carried out using the experimental data that was obtained under laboratory and industrial conditions. The calculated values are in good agreement with the experimental data. The average relative error did not exceed 8%.

We plan to present the results of experimental studies of changes in the properties and composition of the deposit that accumulates in the granular bed in the next article of this series. The results of these studies will be used in the mathematical modelling of physicochemical iron removal from underground water in the water flow compartment of our model. This compartment describes the hydraulics of the granular medium of the filter under the conditions of its progressive clogging.

DATA AVAILABILITY STATEMENT

All relevant data are included in the paper or its Supplementary Information.

REFERENCES

Chaturvedi, S. & Dave, P. N. 2012 Removal of iron for safe drinking water. *Desalination* **303** (1), 1–11. https://doi.org/10.1016/j.desal.2012.07.003.

Deng, Y., Englehardt, J. D., Abdul-Aziz, S., Bataille, T., Cueto, J., De Leon, O., Wright, M. E., Gardinali, P., Narayanan, A., Polar, J. & Tomoyuki, S. 2013 Ambient iron-mediated aeration (IMA) for water reuse. *Water Res.* **47** (2), 850–858. https://doi.org/10.1016/j.watres.2012.11.005.

Du, X., Liu, G., Qu, F., Li, K., Shao, S., Li, G. & Liang, H. 2017 Removal of iron, manganese and ammonia from groundwater using a PAC-MBR system: the anti-pollution ability, microbial population and membrane fouling. *Desalination* **403** (1), 97–106. https://doi.org/10.1016/j.desal.2016.03.002.

Elsehly, E. M. I., Chechenin, N. G., Bukunov, K. A., Makunin, A. V., Priselkova, A. B., Vorobyeva, E. A. & Motaweh, H. A. 2016 Removal of iron and manganese from aqueous solutions using carbon nanotube filters. *Water Supply* **16** (2), 347–353. https://doi.org/10.2166/ws.2015.143.

Galangashi, M. A., Kojidi, S. F. M., Pendashteh, A., Souraki, B. A. & Mirroshandel, A. A. 2021 Removing iron, manganese and ammonium ions from water using greensand in fluidized bed process. *J. Water Proc. Eng.* **39**, 101714. https://doi.org/10.1016/j.jwpe.2020.101714.

Kouzbour, S., Azher, N., Gourich, B., Gros, F., Vial, C. & Stiriba, Y. 2017 Removal of manganese (II) from drinking water by aeration process using an airlift reactor. *J. Water Process Eng.* **16**, 233–239. https://doi.org/10.1016/j.jwpe.2017.01.010.

Luong, V. T., Cañas Kurz, E. E., Hellriegel, U., Luu, T. L., Hoinkis, J. & Bundschuh, J. 2018 Iron-based subsurface arsenic removal technologies by aeration: a review of the current state and future prospects. *Water Res.* **133** (15), 110–122. https://doi.org/10.1016/j.watres.2018.01.007.

Ma, K., Jia, X., Han, H., Zhao, L., Fan, D., Hu, J., Li, R. & Su, X. 2021 Role of typical pipes in disinfection chemistry within drinking water distribution system. *Water Supply* **21** (3), 1263–1276. https://doi.org/10.2166/ws.2020.376.

Madhukar, M., Lavanya, R. S. & Amrutha, M. B. 2013 Defluoridation and deironing of ground water using polystyrene beads. *Water Supply* **13** (6), 1507–1512. https://doi.org/10.2166/ws.2013.116.

Marsidi, N., Hasan, H. A., Rozaimah, S. & Abdullah, S. 2018 A review of biological aerated filters for iron and manganese ions removal in water treatment. *J. Water Process Eng.* **23**, 1–12. https://doi.org/10.1016/j.jwpe.2018.01.010.

Orlov, V., Martynov, S. & Kunytskiy, S. 2016 Energy saving in water treatment technologies with polystyrene foam filters. *J. of Water and Land Develop.* **31**, 119–122. https://doi.org/10.1515/jwld-2016-0042.

Orlov, V., Martynov, S. & Orlova, A. 2017 *Water Preparation on Polystyrene Foam Filters (Pidhotovka Vody na Pinopolistyrolnykh Filtrakh, in Ukrainian)*. National University of Water and Environmental Engineering, Ukraine, p. 175.

Poliakov, V. & Martynov, S. 2021 Mathematical modelling of physicochemical iron removal from groundwater at rapid filters. *Chem. Eng. Sci.* **231**, 116318. https://doi.org/10.1016/j.ces.2020.116318.

Prymushko, S. 2018 *Groundwater State in Ukraine, Yearbook (Stan Pidzemnykh vod Ukrainy, Shchorichnyk, in Ukrainian)*. State Geological Information Fund of Ukraine, Kyiv, Ukraine, p. 121.

Scholz, M. 2016 Chapter 16 - Iron and Manganese Removal. In: *Wetlands for Water Pollution Control*, 2nd edn, pp. 107–109. https://doi.org/10.1016/B978-0-444-63607-2.00016-2

Sharma, S. K. 2009 *Adsorptive Iron Removal From Groundwater. Dissertation for Degree of Doctor*, Delft, The Netherlands, p. 202.

Stiriba, Y., Gourich, B. & Vial, C. 2017 Numerical modeling of ferrous iron oxidation in a split-rectangular airlift reactor. *Chem. Eng. Sci.* **170** (12), 705–719. https://doi.org/10.1016/j.ces.2017.03.047.

Sun, C., Wang, G., Sun, C., Liu, R., Zhang, Z., Marhaba, T. & Zhang, W. 2021 Optimization of iron removal in water by nanobubbles using response surface methodology. *Water Supply* **21** (4), 1608–1617. https://doi.org/10.2166/ws.2021.042.

Tekerlekopoulou, A. G. & Vayenas, D. V. 2008 Simultaneous biological removal of ammonia, iron and manganese from potable water using a trickling filter. *Biochem. Eng. J.* **39** (1), 215–220. https://doi.org/10.1016/j.bej.2007.09.005.

Tugay, A., Oliynuk, O. & Tugay, Y. 2004 *Productivity of Water Intake Well Under Clogging Conditions (Produktyvnist Vodozabirnykh Sverdlovyn V Umovakh Kolmatazhu, in Ukrainian)*. KHAMG, Ukraine, p. 240.

Twort, A. C., Ratnayaka, D. D. & Brandt, M. J. 2006 *Water Supply*, 5th edn. IWA Publishing, London, UK, p. 676.

Vries, D., Bertelkamp, C., Kegel, F. S., Hofs, B., Dusseldorpd, J., Bruins, J. H., de Vet, W. & van den Akker, B. 2017 Iron and manganese removal: recent advances in modelling treatment efficiency by rapid sand filtration. *Water Res.* **109** (1), 35–45. https://doi.org/10.1016/j.watres.2016.11.032.

Water Treatment Handbook 2007, Vol. 2, 7th edn. Set 2007 Lavoisier, Rueil-Malmaison, France, 1904.

First received 13 August 2021; accepted in revised form 28 November 2021. Available online 9 December 2021